Nonlinear latitudinal transfer of wave activity in the winter stratosphere

R. K. Scott

School of Mathematics and Statistics, University of St Andrews, St Andrews, KY16 9SS, UK

*Correspondence to: R. K. Scott, School of Mathematics and Statistics, University of St Andrews, North Haugh, St Andrews, KY16 9SS, UK

The transfer of wave activity between wave guides separated in latitude by a surf zone region of zero potential vorticity gradient is investigated in a simple model of the winter stratosphere and its extension into the tropics. The distinction from classical wave propagation on a slowly varying background state is illustrated in a conceptual model in which latitudinal separation is reduced locally by wave disturbances of finite amplitude, impling a nonlinear dependence of the transfer on wave amplitude and a nonlinear transfer of wave activity to higher zonal wavenumbers. The response of a topographically forced vortex in the presence of different forms of tropical circulation, comprising either uniform or vertically localized anomalies, is examined numerically, using an exact pseudomomentum based wave activity to diagnose separately the vortex and tropical wave responses. Changes to the zonal mean flow in the tropics are related in a natural way to the potential vorticity structure of the background state and the associated wave guides, which also control the general character of tracer mixing across and out of the tropics.

Key Words: planetary wave, potential vorticity, wave guide, nonlinearity

This article has been accepted for publication and undergone full peer review but has not been through the copyediting, typesetting, pagination and proofreading process, which may lead to differences between this version and the Version of Record. Please cite this article as doi: 10.1002/qj.3536

1. Introduction

Matsuno's (Matsuno 1970) refractive index of the zonal mean zonal velocity provides a useful indication of Rossby wave propagation in the winter stratosphere. It is defined, under the quasi-geostrophic approximation by

$$n_s^2 = \frac{\bar{q}_\phi}{a(\bar{u}-c)} - \frac{s^2}{a^2\cos^2\phi} - \frac{f^2}{4N^2H^2}, \qquad (1)$$

where $\bar{q}$ is the zonal mean quasi-geostrophic potential vorticity, $\bar{u}$ is the zonal mean zonal velocity, s is the zonal wavenumber and other variables have their standard definitions. Perturbations to the zonal mean flow will tend to propagate upgradient of n_s^2 and are evanescent in regions where $n_s^2 < 0$, in a description analagous to that of geometric optics. In the absence of any mean flow, the latitudinal variation of n_s^2 implies that waves will tend to propagate to low latitudes, an effect that is more pronounced at higher zonal wavenumbers (Karoly and Hoskins 1982), and which accounts in part for the dominance of planetary wavenumbers in the winter polar stratosphere. On the other hand, wave propagation is enhanced in regions of strong latitudinal gradient of potential vorticity, $\bar{q}_\phi$, such as typically occur on the polar vortex edge, which may act as a wave guide for upward propagating waves (Simmons 1974).

In contrast to the situation of geometric optics, however, in the winter stratosphere there may be little or no scale separation between waves and mean flow, in either horizontal or vertical directions; observed vertical wavelengths may exceed the depth of the entire stratosphere, while often a meaningful latitudinal wavelength is difficult to define. While lack of scale separation and the typically large amplitudes of disturbances presents a violation of the fundamental assumptions underlying the theory, the refractive index has been widely adopted and indeed performs remarkably well, well outside its expected domain of validity. Nonetheless, the lack of scale separation prompts the question of whether other useful diagnostics may be more appropriate in certain situations, or under certain dynamical conditions.

An example of such a situation is the category of stratospheric sudden warming events that are characterized by a strong zonal wavenumber two disturbance, in which the vortex is observed to split into two lobes throughout the depth of the stratosphere. The largely barotropic structure of these events was documented by Matthewman *et al.* (2009) and the fixed orientiation of the splitting is further indication that the response is to a geographically stationary wave forcing. The identification and theory for the resonant excitation of such a barotropic mode goes back to Tung and Lindzen (1979a,b) and Plumb (1981) and was developed for the specific geometry of the winter polar stratosphere by Esler and Scott (2005); see also Esler *et al.* (2006), Matthewman and Esler (2011), Albers and Birner (2014), Liu and Scott (2015), Scott (2016) for further refinements and applications. The barotropic structure of this mode implies infinite vertical wavelength, and it appears in linear theory as an external mode, lying outside the continuous spectrum of vertically propagating waves of the theory of Charney and Drazin (Andrews *et al.* 1987). For conditions most relevant to middle and late winter, when the vortex is well-defined and potential vorticity well-mixed in latitude across the surf zone, waves are confined to the vortex edge and evanescent in latitude. In the theoretical development of Esler and Scott (2005) (hereafter ES05), this latitudeal confinement was exploited to obtain exact expressions for the vortex response to a given forcing. It also made clear that the only relevant flux of wave activity was that in the vertical direction, since zero potential vorticity gradients in the surf zone (which extended without latitudinal bound in that model) did not allow for any latitudinal wave propagation or transfer of wave activity away from the vortex edge.

Although the model employed by ES05 and subsequent studies, with an infinitely sharp vortex edge and perfectly mixed surf zone, provides an appropriate framework in which to examine vertical wave propagation and resonant excitation, to the extent that the actual vortex edge is sharp

and the surf zone well mixed, it omits a transition to low potential vorticity values that necessarily occurs in the real atmosphere. It therefore precludes altogether the possibility of lateral wave propagation, which must occur to some extent in the winter stratosphere, if only by the nonlocality of the potential vorticity inversion operation, and if in a manner more involved than can be represented by (1).

In this paper, we provide a tentative description of how lateral wave propagation or, perhaps more appropriately, a transfer of wave activity, may occur between the polar vortex edge and the tropics in the situation where (i) the polar vortex edge is sharp, (ii) the surf zone is well-mixed, and (iii) where the tropical potential vorticity distribution consists of some transition from surf zone to background planetary gradient. Regarding (iii), such a transition may take a variety of forms and may depend, among other things, on details such as the phase of the tropical quasi-biennial oscillation (QBO), the time within the winter evolution, and the height within the stratosphere. However, the tendency for steep potential vorticity gradients to develop on the equatorward edge of the surf zone is well-known and dynamically understood (Juckes and McIntyre 1987; Polvani *et al.* 1995), so some form of wave guide in the tropics is expected. We also provide a quantitative analysis, albeit within a highly idealized model configuration, of how different perturbations to the low-latitude potential vorticity distribution influences the transfer of wave activity between the polar vortex edge and the tropics, and how this transfer affects the evolution of the vortex itself. Some speculation on the implications for the Holton–Tan effect, the observed correlation between QBO phase and strength of the winter vortex, (Holton and Tan 1982; Dunkerton 1991) are given, to the limited extent allowed by the model simplifications.

2. Lateral transfer of wave activity between wave guides

Our framework for lateral wave activity transfer in the winter stratosphere is based on an idealization of the dominant potential vorticity distribution of the winter stratosphere, in which the wave guides of the polar vortex edge and low-latitude edge of the surf zone are represented by sharp jumps, separating regions of uniform potential vorticity in the polar vortex, surf zone, and tropical regions. The use of this type of idealization is based on the early insights of Simmons (1974) and well-established in the literature (e.g. Dritschel and Saravanan 1994; Waugh and Dritschel 1999), while the effect on vertical propagation of smoothing a sharp vortex edge has also been considered (Scott *et al.* 2004). Waves are considered to originate at the surface or in the troposphere, and be either upward propagating on the vortex edge or barotropic and non-propagating in the vertical as described in ES05. We are predominantly interested in the transfer of wave activity across the surf zone, from the vortex edge to a tropical wave guide or beyond. The zero potential vorticity gradients in the surf zone clearly imply that the traditional concept of wave propagation, in the sense of perturbations to a spatially homogeneous background, is inappropriate. In the proposed scenario, waves are trapped on the wave guides and evanscent in latitude, but can bridge the gap between vortex edge and tropical wave guide due to the nonlocality of potential vorticity inversion. We may thus think of two extremes: on the one hand, continuous wave propagation in the traditional sense, involving wave packets on a slowly varying background flow, in which concepts such as Matsuno's refractive index are meaningful—upward propagating waves are refracted equatorward according to the curvature in the background flow; on the other hand, a nonlocal transfer of wave activity between wave guides, motivated by the nonlocality of potential vorticity inversion. No complete theory has been developed for the latter case, although in the linear limit concepts of Rossby wave phase and group propagation can be formulated, considering the edge wave case as an extreme discretization of the continuous one (Zhu and Nakamura 2010). The different pictures may be more or less relevant under different winter conditions. In early winter, for example, potential vorticity gradients are relatively weak: steep gradients at the polar

vortex edge are yet to develop, and the traditional paradigm may be the more appropriate. The other extreme of lateral wave transfer between wave guides may be more relevant in mid-late winter, once the vortex edge and surf zone are better defined.

Even in the idealized case where the surf zone is perfectly mixed and potential vorticity gradients are identically zero, transfer of wave activity across it from the polar vortex edge to tropical edge will occur simply due to the nonlocality of potential vorticity inversion. A small amplitude wave on the polar vortex edge will induce a wave on the tropical edge with amplitude approximately inversely proportional to the exponential of the width of the surf zone, since the flow induced by a PV disturbance decays exponentially with distance. Wave transfer in this case is weak but linear, in the sense that doubling the amplitude of the wave on the polar vortex edge doubles the amplitude of the wave induced on the tropical edge.

Nonlinearity becomes important when the amplitude of the wave on a vortex edge becomes comparable to the width of the surf zone. In that case, the potential vorticity anomaly due to such a wave is brought closer to the subtropical edge, locally reducing the distance across which inversion must apply. Thus the proximity of the vortex edge wave acts to enhance nonlinearly the transfer of wave activity to the tropical edge. Additionally, becauce the enhancement due to the proximity occurs over a limited range in longitude, there is a transfer of wave activity from lower to higher zonal wavenumber, an inherently nonlinear transfer. The schematic shown in Figure 1 illustrates these concepts: in panel (a), the nonlocality of potential vorticity implies a weak transfer of wave activity from a small-amplitude vortex edge wave; in panel (b) the vortex edge is brought closer to the tropical edge locally in longitude and as a result excites waves more strongly over a restricted longitudinal range, and with consequently higher zonal wavenumber. Note that even in the case (a), where there is a purely linear transfer of wave activity, waves are not propagating in the usual sense.

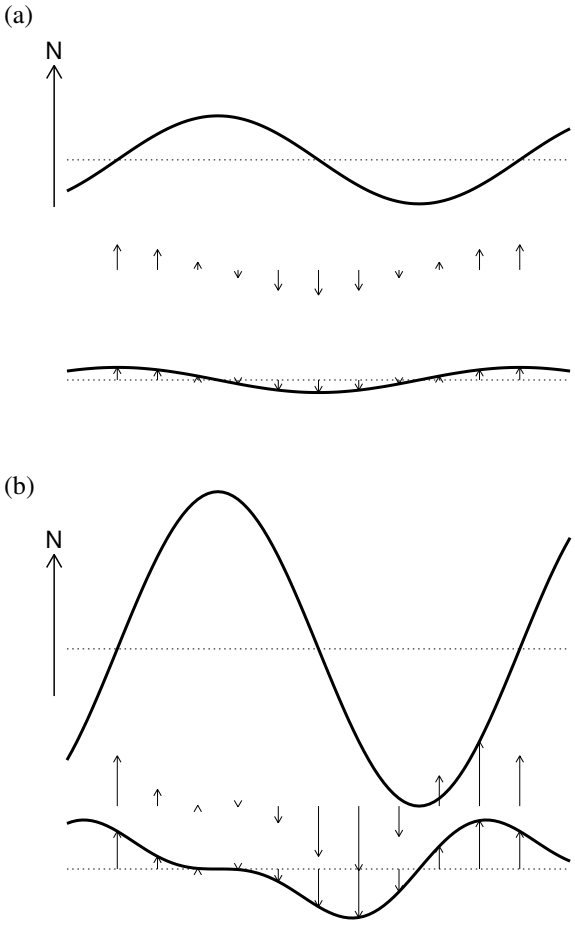

Figure 1. (a) Linear wave dynamics: a small amplitude wave on the vortex edge (top line) induces a perturbation on the tropical edge of the surf zone (lower line). The perturbation decays exponentially with the width of the surf zone and is linear in the sense that the response amplitude varies linearly with the amplitude of the vortex wave and has the same zonal wavenumber. (b) Finite amplitude effect: a large amplitude wave on the vortex edge reduces the distance between vortex and subtropical edge locally, resulting in a local increase of response amplitude beyond linear scaling and an increase in the zonal wavenumber of the excited response.

3. Model description

The quasigeostrophic equations for a compressible atmosphere form a convenient system in which to study the above effects. Potential vorticity can be specified in a simple and controllable way and the evolution is govenerned by simple material advection. The equations are

$$\frac{\partial q}{\partial t} + \mathbf{u} \cdot \nabla_h q = 0 \tag{2}$$

where the horizontal velocity $\mathbf{u}$ has a streamfunction ψ obtained from q via the inversion operator,

$$\nabla_h^2 \psi + \frac{1}{\rho_0} \frac{\partial}{\partial z} \left(\rho_0 \frac{f_0^2}{N^2} \frac{\partial \psi}{\partial z} \right) = q - f. \tag{3}$$

The lower boundary condition for (3) is $\psi_z = -N^2 h_0/f_0$, representing flow over variable topography h_0. Here N is a uniform buoyancy frequency, $\rho = e^{-z/H}$ is the density, H is a density scale height, f is a variable Coriolis parameter, and f_0 its value at the pole. Physical parameter values are $f_0 = 2\Omega = 4\pi/\text{day}$, while $H = 7544\,\text{m}$ is chosen such that the deformation radius, $L_D = NH/f_0 = \sqrt{g\kappa H}/f_0 = 1000\,\text{km}$.

To evolve the system (2) efficiently, the field q is represented by a set of contours that are advected by the corresponding flow field, using the CASL algorithm of Dritschel and Ambaum (1997). We use a simplified cylindrical geometry with polar γ-plane representation of the background planetary potential vorticity $f(r) = f_0(1 - \frac{1}{2}\gamma r^2)$, where γ is a constant coefficient (Macaskill *et al.* 2003; Scott *et al.* 2004). We consider the radius r as representing the distance from the pole, be proportional to colatitude $\phi^c = 90^\circ - \phi$, and identify the equator, $\phi = 0$, with the radius r_{eq} at which $f(r) = 0$. Thus $\gamma = 2/r_{eq}^2$ and, with the above choice $L_D = 1000\,\text{km}$, it is appropriate to set $r_{eq} = 10L_D$. Defining γ in this way slightly underestimates, by a factor $8/\pi^2 \approx 0.81$, the actual variation in f over a spherical pole obtained from an expansion of $2\Omega\sin\phi$. The lateral boundary of the domain is set at $r = 15L_D$, far enough distant to have negligible influence on the dynamics of interest. The vertical depth of the model is taken to be $8H$.

The initial conditions are as follows. A polar vortex is represented by a horizontally circular patch of quasigeostrophic potential vorticity, of radius $r_v = 4L_D$, centred on the origin, and extending uniformly in height, following Dritschel and Saravanan (1994); Scott *et al.* (2004) and ES05. It is surrounded by a surf zone region of constant q. At "low-latitudes", the potential vorticity transitions from the surf zone value to the planetary value in one of three ways, as depicted in Fig. 2: a control case with zonal wind equal zero across the tropics, and cases with easterly and westerly tropical anomalies. In the easterly case, q is taken to be completely mixed across the equator between a northern subtropical edge at $r = r_N = 8L_D$ and its southern counterpart $r = r_S$, defined by $r_S^2 - r_{eq}^2 = r_{eq}^2 - r_N^2$ so that the areas on either side of the equator are the same. Note that unlike full spherical geometry, $r_N - r_{eq} \neq r_{eq} - r_S$, although the difference between the two is small. In the westerly case, potential vorticity is taken to be mixed on either side of r_{eq}, again out to r_N and r_S, in such a way that the value on the northern side takes the same value as that in the surf zone, in other words, the surf zone extends all the way to the equator. On the southern side, the potential vorticity takes the negative of this value, consistent with an area preserving rearrangement between the northern and southern flanks, following the potential vorticity staircase constructions of Dunkerton and Scott (2008); Dritschel and McIntyre (2008).

In terms of latitudes corresponding to the above transition radii, the complete specification of potential vorticity in the three cases is given by

$$q_c(\phi) = \begin{cases} q_v & \phi_v \le \phi \le 90^\circ \\ q_z & \phi_N \le \phi < \phi_v \\ f(\phi) & \phi < \phi_N \end{cases} \tag{4}$$

$$q_E(\phi) = \begin{cases} q_v & \phi_v \le \phi \le 90^\circ \\ q_z & \phi_N \le \phi < \phi_v \\ 0 & \phi_S \le \phi < \phi_N \\ f(\phi) & \phi < \phi_S \end{cases} \tag{5}$$

$$q_W(\phi) = \begin{cases} q_v & \phi_v \le \phi \le 90^\circ \\ q_z & 0 \le \phi < \phi_v \\ -q_z & \phi_S \le \phi < 0 \\ f(\phi) & \phi < \phi_S \end{cases} \tag{6}$$

where ϕ_v is the vortex edge, ϕ_N is the subtropical extent of the surf zone, and ϕ_S is the corresponding latitude in the southern hemisphere. The surf zone value, q_z, is defined so that $q_c(\phi)$ is continuous at ϕ_N and the jump at the vortex edge, $\delta q_v = q_v - q_z$, is defined so that the

zonal wind corresponding to $q_c(\phi)$ is zero for $\phi < \phi_N$. The model framework allows for different profiles to be prescribed on different vertical levels, although most of the results described in the next section are for a uniform vertical structure, this being the simplest possible setting in which to examine the latituduninal transfer of wave activity. Generalizations to non-trivial vertical structure in both the polar vortex and the tropical anomalies can be considered within the same framework (see, for example Esler *et al.* 2006) but complicate the interpretation of the dynamics. The three profiles are shown in Fig. 2 with the various transition latitudes indicated. To make clear the area preserving nature of the perturbations, we have used $(\phi^c)^2 \propto r^2$ as the horizontal coordinate, the cylindrical equivalent of the coordinate $\mu = \sin\phi$ typically used in spherical geometry. While clearly a gross oversimplification, the profiles nevertheless capture the basic stratospheric wave guides of the vortex edge and subtropical flank of the surf zone (Juckes and McIntyre 1987; Polvani *et al.* 1995; Scott and Liu 2015).

The jumps in q at ϕ_v, ϕ_N, 0 and ϕ_S are represented by a single contour on each vertical level. The continuous, quadratic background profile is represented by a discrete set of γ-contours. In the case of q_c there are 11 contours equally spaced in area between ϕ_N and ϕ_S; beyond ϕ_S these are continued with the same spacing in area to the domain boundary.

Wave are excited on this initial state in a manner very similar to that of ES05. Specifically, we define a topographic height of the form

$$h_0 = h_b H g(\phi) f(t) \cos k\lambda,$$

where k is the zonal wavenumber, λ is longitude, $g(\phi)$ and $f(t)$ are specified functions of latitude and time respectively, and h_b is a dimesionless topographic amplitude. Here we take $k = 2$.

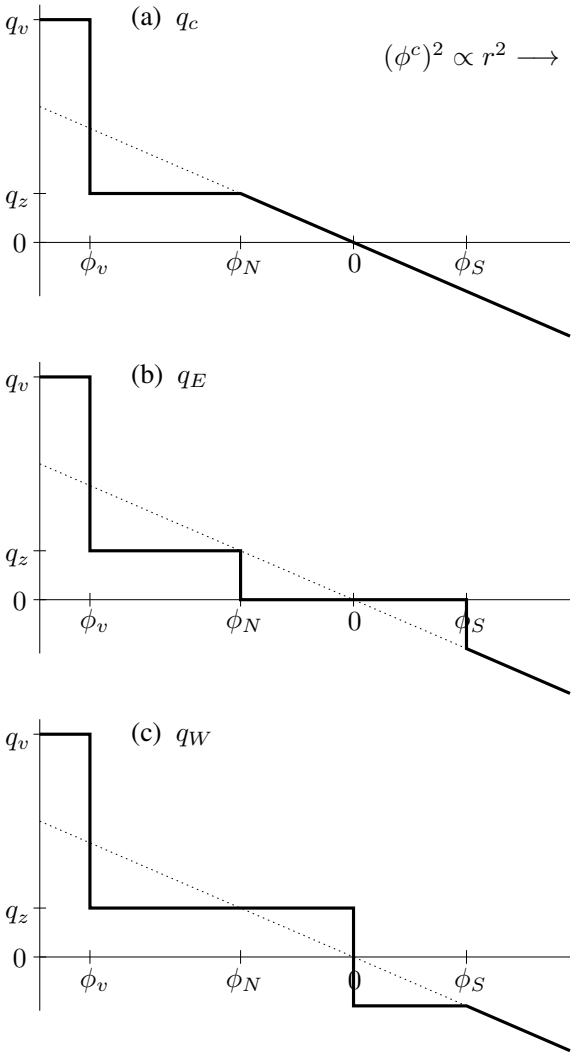

Figure 2. The three profiles, (a) control, (b) easterly perturbation, and (c) westerly perturbation, defined by (4), (5), and (6), respectively. The profiles are plotted against the area coordinate r^2 with the transition latitudes indicated.

The function $f(t)$,

$$f(t) = e^{-t^2/T^2} e^{i(k\lambda - \omega_b t)}$$

represents a gaussian pulse of width T, centred on $t = 0$ and with frequency ω_b in the zonal direction, i.e. eastward travelling phase speed ω_b/k. In frequency space it corresponds to a gaussian distribution of frequencies with width $2\pi/T$, centred on ω_b. Here we take $T = 2$ days, while integrations start at $t = -10$ days and terminate at $t = 10$ days; the forcing is therefore negligible at the beginning and end of the integrations. As in ES05, we consider a range of values of ω_b that excites the full spectrum of vertically propagating waves and the external mode.

The function $g(\phi)$ is the truncated Bessel function,

$$g(\phi) = \begin{cases} J_k(\phi^c l/\phi_0^c) & \phi > \phi_0 \\ 0 & \phi < \phi_0 \end{cases}$$

where ϕ_0 is the latitudinal extent of the forcing and l is the first zero of J_k. We take $\phi_0 = \phi_N$ so that the forcing is effectively confined to the latitudes of the polar vortex and surf zone and does not project significantly into the tropics.

4. Results

We present two series of experiments. In the first, sections 4.1–4.2, the initial potential vorticity takes the latitudinal forms (4)–(6) uniformly in height; in other words, the tropical easterly or westerly pertubations are applied throughout the depth of the stratosphere. In the second, section 4.3, the tropical perturbations are prescribed in a limited range of vertical levels, $H \leq z \leq 3H$, intended as a crude representation of the potential vorticity anomalies of the QBO.

4.1. Polar vortex response

We look first at the influence of the low-latitude potential vorticity distribution on the polar vortex response. Specifically, we consider the vortex response as a function of forcing frequency for the three initial potential vorticity profiles (4)–(6). The control case is similar to the case examined by ES05, with differences due to the finite extent of the surf zone and the transition to background planetary vorticity beyond it. Following ES05, we measure the vortex response to the forcing in terms of the total change in angular momentum of the system, equal to the time integrated Eliassen-Palm flux through the lower boundary:

$$\Delta M = -\int_{-\infty}^{\infty} F|_{z=0}(t)dt. \qquad (7)$$

Conservation of angular pseudomomentum implies this is equal to the negative of the total wave activity $\mathcal{A}$, where the latter is a fully nonlinear quantity proportional to the total area displacement of the potential vorticity contours from their initial axisymmetric configuration (Dritschel and Saravanan 1994)—see ES05 for a complete discussion in the current context. A similar area-based wave activity has also been considered by Nakamura and Zhu (2010) and extended to the global primitive equations byNakamura and Solomon (2011).

When analyzing the vortex response to the forcing, as well as the transfer of wave activity between the vortex and the tropics, it is convenient to decompose (7) into a contribution $\mathcal{A}_v$ due to wave perturbations to the vortex edge and a contribution $\mathcal{A}_t$ due to wave perurbations to the potential vorticity contours lying initially in the low-latitude region $\phi < \phi_N$, south of the polar vortex and surf zone. We then define the vortex response $\Delta M_v = -\mathcal{A}_v$, the change in angular momentum associated with the wave perturbation of the vortex edge.

The vortex response for the control case is shown in Fig. 3 for a range of forcing frequencies, ω_b, and forcing amplitudes $h_b = 0.05, 0.1, 0.2, 0.4$. Each symbol represents a different simulation and is plotted at a position corresponding to the total change ΔM_v over the length of the integration. Values have been normalized by the square of the forcing amplitude, h_b, and by the initial vortex angular impulse, $\mathcal{J}_0$, to enable comparison on a single graph. The form of the response is qualitatively similar to that obtained by ES05 (Fig.4 therein). With weak forcing, $h_b = 0.05$ and $h_b = 0.1$, the wave response is approximately linear in forcing amplitude, so that the vortex wave activity scales quadratically with forcing amplitude; thus the curves of the normalized response are approximately overlapping at low h_b. With stronger forcing, there is a departure from linear scaling in the sense that larger forcing amplitudes are proportionately less efficient at exciting waves on the vortex edge.

The approximately gaussian shape of the response at small h_b reflects the gaussian frequency distribution of the forcing and the fact that for most frequencies the vortex response is dominated to a large extent by the

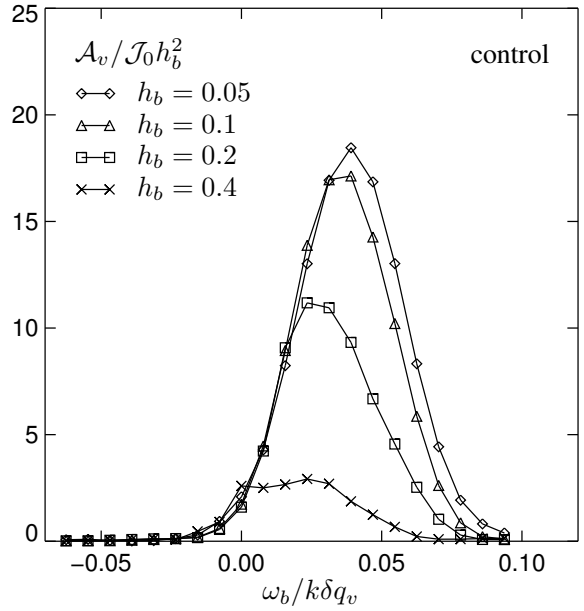

Figure 3. Normalized vortex response for the control case with initial potential vorticity given by (4) uniformly in height. Symbols indicate different forcing amplitudes as indicated. The quantity $\mathcal{A}_v/\mathcal{J}_0 h_b^2$ represents the total wave activity of the vortex contour, normalized by the forcing amplitude, h_b, at the final time of each simulation $t = 10$ days. Other physical parameters, ω_b, k, and δq_v, are as described in section 3.

barotropic mode (see ES05 section 3b, and compare solid and dotted lines in ES05 Fig.4). Thus the gaussian shape of the response predominantly reflects the degree to which the forcing distribution projects onto the frequency of the barotropic mode. Note that due to the more complicated latitudinal potential vorticity structure used here, and the corresponding presence of Rossby wave critical latitudes, it is impractical to determine the precise frequency limits of the barotropic and Charney-Drazin modes.

At larger h_b, there is a reduction in the (normalized) vortex response and a shift to lower frequencies of the peak response. Both are due to weakly nonlinear effects: at large amplitude a significant deceleration of the vortex accompanies the growth of the wave, which alters the effective resonant frequency of the vortex relative to the forcing. In other words, forcing at the resonant frequency will result in a vortex deceleration that detunes the vortex from resonance. For optimal excitation of the vortex it is necessary to force the vortex at a more negative frequency, so that deceleration of the vortex acts to bring the system closer to resonance, the self-tuning mechanism of Plumb (1981). Note that the reduction in magnitude of the response

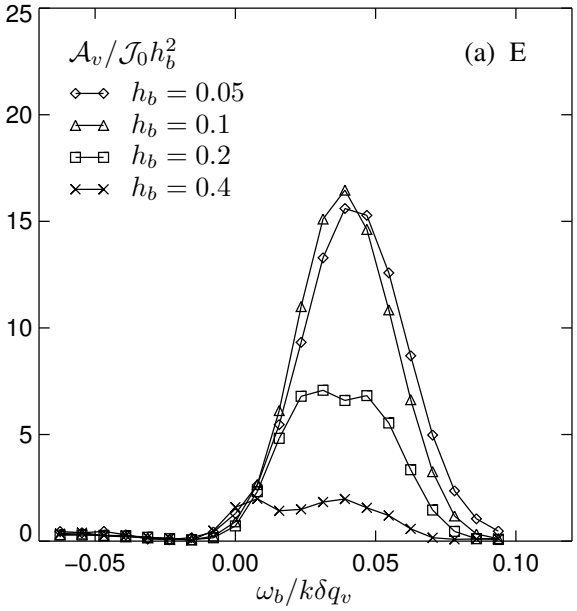

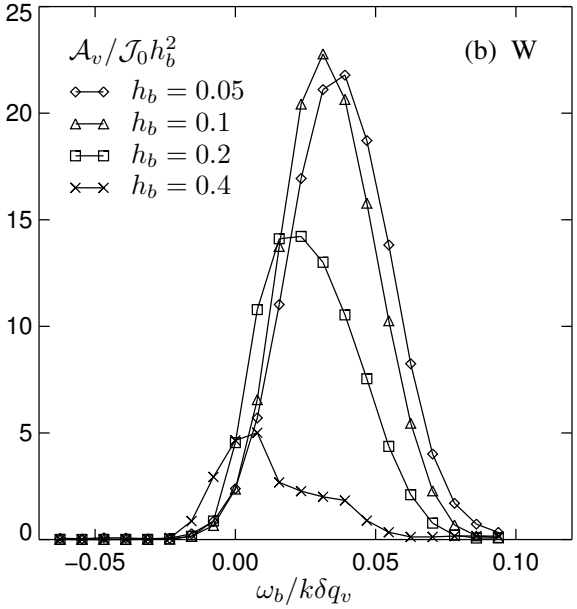

Figure 4. As Fig. 3, but for (a) an easterly tropical anomaly, uniform in height, with initial potential vorticity given by (5) and (b) an westerly tropical anomaly, uniform in height, with initial potential vorticity given by (6).

at larger h_b is similar to that found in ES05, but significantly more pronounced.

The vortex responses for the two pertubation cases in which the initial vorticity profile is given by either (5) (tropical easterly anomaly) or (6) (tropical westerly anomaly), uniformly in height, are shown in Fig. 4. There is a clear reduction in the strength of the vortex response in the tropical easterly case, for all four forcing amplitudes, and enhancement of the vortex response in the tropical westerly case. The location of the peak response, indicating

the frequency of the barotropic mode, is virtually unchanged in both cases, which may be expected since the vortex parameters themselves are the same in all cases.

Part of the change in the vortex response may be attributed to changes in the amount of wave activity transferred from the polar vortex edge to the tropics, as described in the next section. However, this transfer cannot fully account for the difference seen in Fig. 4. Note that the change in the vortex response is not due to any changes in the initial vortex state itself, which by construction is identical in all three cases considered. In fact the entire zonal mean zonal wind profile north of ϕ_N is the same in each case. However, the horizontal structure of the free modes existing on the vortex edge depends nonlocally on the global potential vorticity distribution, and therefore varies between the cases. The extent to which the topographic forcing, which has fixed latitudinal structure, projects onto and hence excites the vortex wave modes, therefore also varies between cases. The result of this effect is linear in forcing amplitude but is distinct from the issue of latitudinal propagation.

4.2. *Transfer of wave activity into the tropics*

We next consider the response in the tropics, diagnosed primarily by the total wave activity at end of each calculation due to all potential vorticity contours initially in the region south of ϕ_N. Recall that the topographic wave forcing is restricted to latitudes $\phi > \phi_N$ and excites waves predominantly on the vortex. Thus the primary source of wave activity in the tropics involves lateral transfer of wave activity from the vortex through the surf zone.

Fig. 5 shows the tropical response for the control case, for the same set of forcing parameters as described above, while Fig. 6 shows the tropical response for the easterly and westerly pertubation cases. Considering first the control case, there are two main features of the response. First, the structure of the response across forcing frequencies is very different to that of the vortex response, with a distint two-peak structure. It turns out that the left-most peak, near

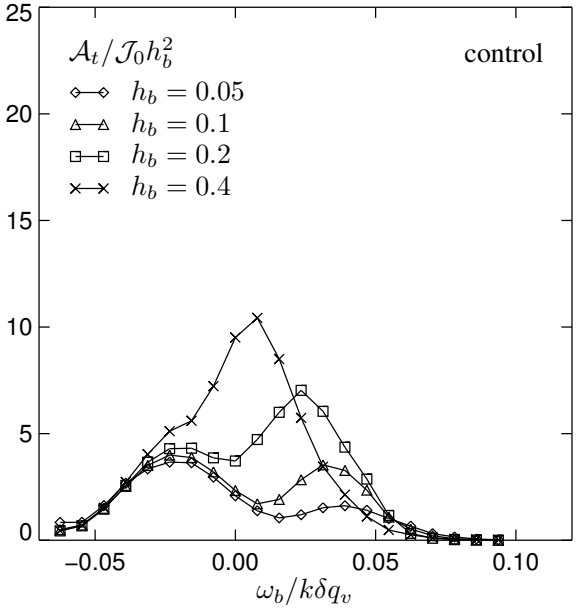

Figure 5. As Fig. 3 but the tropical response: wave activity associated with potential vorticity contours initially located at $\phi \leq \phi_N$ (all potential vorticity contours excluding the polar vortex).

frequency $\omega_b/k\delta q \approx 0.025$, is due to a direct excitation of waves on the background planetary potential vorticity field in the tropics by the topographic forcing, even though the latter is well separated in latitude. Indeed, at these forcing frequencies the vortex response is very small, as can be seen in Fig. 3; inspection of the potential vorticity fields (not shown) also confirms that the vortex waves are extremely small in these cases. More importantly, the scaling of the tropical response at these frequencies is approximately quadratic in forcing amplitude, i.e., wave amplitude varies linearly with forcing amplitude, consistent with a direct role of the topographic forcing.

The left most peak in the response alters significantly in the perturbation experiments, with an enhancement and shift to more negative frequencies under the easterly perturbation and an almost complete disappearance under the westerly perturbation. The shift to more negative (easterly) frequencies under the easterly perturbation is consistent with the sense of the change in the tropical winds. However, reasons for the changes in magnitude of the response under both perturbations are more subtle and linked to the detailed position of the potential vorticity gradients of the basic state. The potential vorticity fields near the end of the integrations (not shown, but similar to

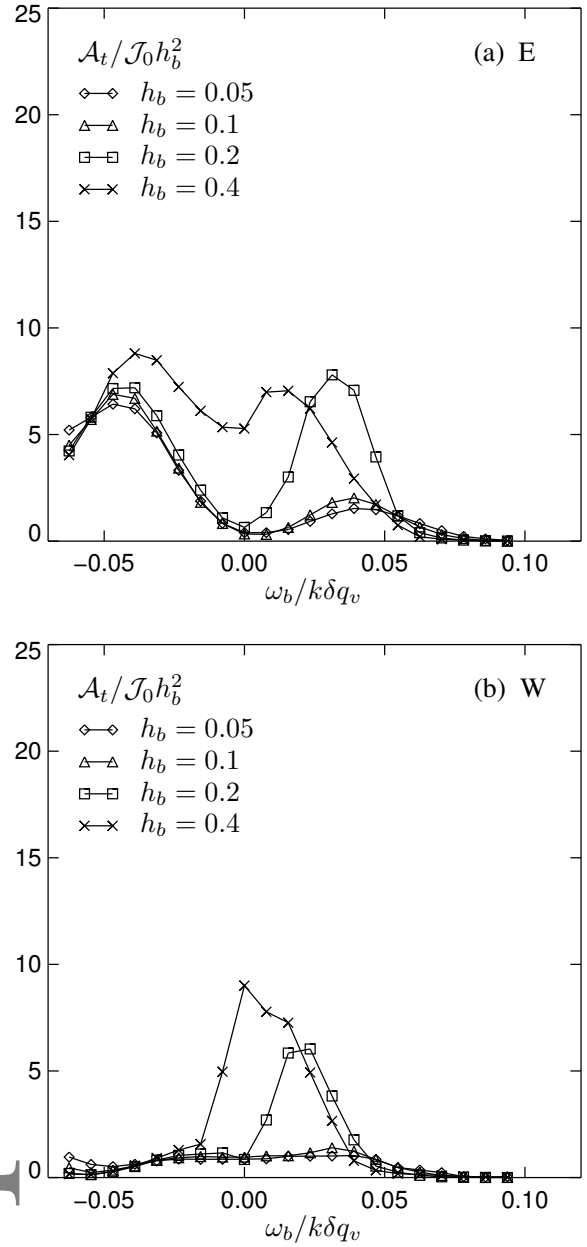

Figure 6. As Fig. 4 but the tropical response: wave activity associated with potential vorticity contours initially located at $\phi \leq \phi_N$

other examples discussed below) indicate that the strongest mixing of potential vorticity is in the subtropics, closest to the terminus of the forcing. Under the easterly perturbation, there is a large potential vorticity gradient right at ϕ_N, whereas under the westerly perturbation potential vorticity gradients are zero all the way to the equator. Mixing of air in the latter case, therefore, makes no contribution to the wave activity. The background planetary vorticity contours of the control cases are somewhere inbetween these extremes.

The second main feature of the response, and the main point of interest here, is the nonlinear scaling of the rightmost peak. Notice that the magnitude of the response, which is normalized by h_b^2, increases with increasing h_b. Linear scaling would result in the curves overlapping as in the case of the leftmost peak. The increase in normalized response magnitude with forcing amplitude indicates a superlinear scaling. Further, the peak of the response corresponds closely to the peak in the vortex response discussed above. Combined, these results suggest that the origin of the tropical response here involves the lateral transfer of wave activity from the vortex edge to the tropics, with the superlinear scaling consistent with the finite amplitude reduction in separation between vortex edge and tropics, as was illustrated schematically in Fig. 1. In support of this, Fig. 7 shows potential vorticity at $t = 0$ days (the time of the peak forcing amplitude) at a representative vertical level (the response is mostly uniform in height) for three forcing amplitudes $h_b = 0.1, 0.2, 0.4$ and forcing frequency $\omega_b/k\delta q \approx 0.031$. The forcing frequency corresponds approximately to the peak in the tropical response, noting that at this early time, the effects of weakly nonlinear detuning of the vortex are small. The locally enhanced proximity of the vortex edge to the tropical potential vorticity is clearly visible at higher forcing amplitude, and a greater than twofold increase in wave amplitude is particularly clear between the cases $h_b = 0.2$ and $h_b = 0.4$.

Although the tropical responses at positive frequencies (those near the frequency of the barotropic response) are similar between the easterly and westerly perturbation cases, for example, the $h_b = 0.2$ line in Fig. 6, there are important differences in details of the potential vorticity evolution. Fig. 8 shows three snapshots of the potential vorticity for the easterly and westerly perturbation cases with $h_b = 0.2$ and $\omega_b/k\delta q \approx 0.023$ (near the peak of the tropical response for both cases) between $t = 2$ and $t = 6$ days after the peak forcing, and at a representative height of $z = 2H$ (again, the response is nearly uniform in height in all cases). Contours with strong potential vorticity jumps, initially located at ϕ_v, ϕ_N, 0, and ϕ_S, are indicated bold. As

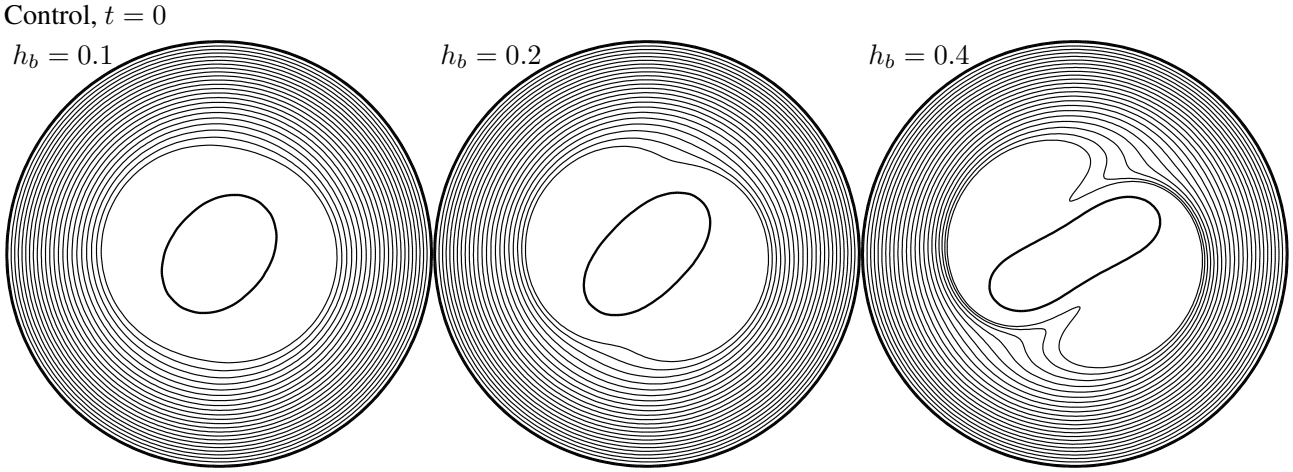

Figure 7. Potential vorticity at $z = 2H$ and $t = 0$ days (peak forcing time) from the control case with forcing frequency $\omega_b/k\delta q \approx 0.031$ and forcing amplitudes $h_b = 0.1, 0.2, 0.4$ (left to right). The contour at the polar vortex edge is in bold; thin contours represent the background γ-plane potential vorticity.

before, there is a significant elongation of the polar vortex, spanning the width of the surf zone and bringing the vortex edge locally into closer proximity to the tropical potential vorticity. In comparison, note for example that the bold contours at ϕ_N and ϕ_S in panels (a) remain well separated, and the substantial wave activity on the contour at ϕ_N has no visible effect on the contour at ϕ_S.

The nature of advective mixing in the tropics and surf zone is markedly different between the two cases and consistent with studies of the influence of the QBO on tropical mixing based on effective diffusivity calculations using meteorological reanalysis (Shuckburgh *et al.* 2001; Abalos *et al.* 2016). The Lagrangian picture afforded by the potential vorticity evolution indicates additionally the direction of mixing in various regions. In the easterly case, the subtropical edge at ϕ_N (bold) is strongly distorted into the surf zone and mixed across the entire region, with a collapse of scales into narrow filamentary debris. However, only this contour experiences such strong mixing. Tracer contours (thin light) south of ϕ_N remain relatively undisturbed and there is very little mixing of most of the tropical region into the surf zone. In the westerly case, in contrast, air from the entire northern tropical region, $0 < \phi \leq \phi_N$ is mixed into the surf zone. These tracer contours have zero potential vorticity jump and do not contribute to the wave activity. South of the equator, air is again mixed within the region $\phi_S < \phi < 0$. However, there is no mixing across the equatorial potential vorticity jump itself, in agreement with the highly localized equatorial minimum of effective diffusivity found by Shuckburgh *et al.* (2001) and Abalos *et al.* (2016). The equatorial contour experiences significant distortion but remains undular and non-filamenting, as might be expected from permeability considerations (Dritschel and McIntyre 2008), while its undulations are responsible for most of the tropical response in wave activity.

The nonlinear nature of the wave activity transfer is apparent in the higher zonal wavenumbers of the induced equatorial wave: see Fig. 8(b) at times $t = 4, 6$. Note that these higher wavenumbers can only arise from the proximity mechanism described here and illustrated schematically in Fig. 1; in particular, the higher wavenumbers cannot be the result of any kind of shear instability, barotropic or baroclinic, since the potential vorticity distribution remains monotonic in latitude at all levels throughout the evolution. A phase lag can be observed as the orientation of the vortex rotates eastward throughout this period, exciting waves on the tropical wave guide as it goes.

A similar difference in the character of mixing between easterly and westerly perturbations is also found at higher forcing amplitudes (not shown). The easterly case with

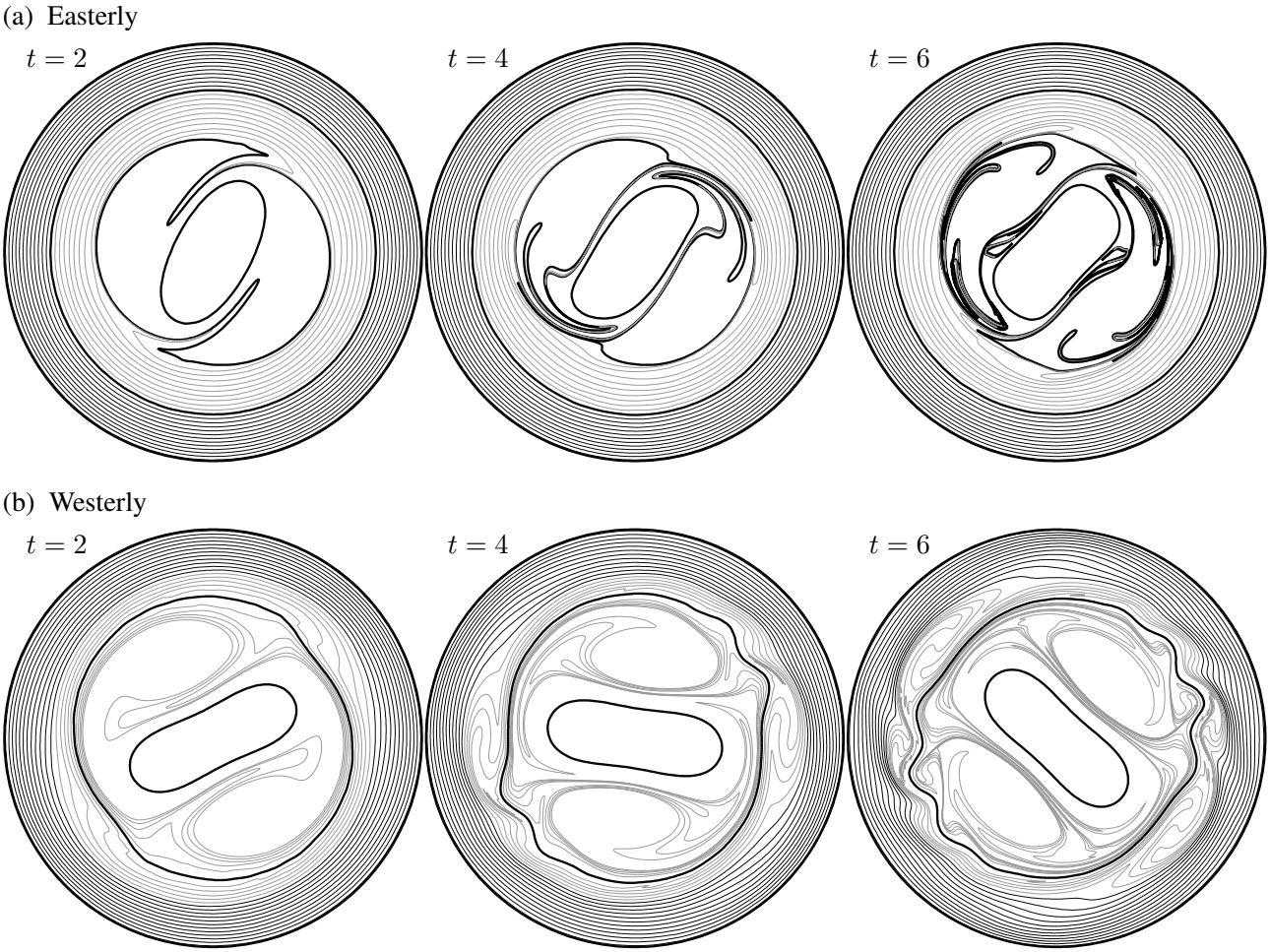

Figure 8. Potential vorticity at $z = 2H$ at $t = 2, 4, 6$ days for the case $h_b = 0.2$ and $\omega_b/k\delta q \approx 0.0234$ and (a) easterly perturbation (b) westerly perturbation. Contours with strong potential vorticity jumps, at ϕ_v, ϕ_N, 0, and ϕ_S, are indicated bold. Thin black contours represent the background γ-potential vorticity. Thin gray contours, initially between ϕ_N and ϕ_S represent a passive tracer only, with no potential vorticity jump across them.

$h_b = 0.4$ and $\omega_b/k\delta q \approx 0.008$, again near the peak in tropical wave activity, is broadly similar to Fig.8(a) but with more vigorous mixing into the surf zone. There is only very weak mixing in the tropics and again no significant wave excitation at ϕ_S. In the corresponding westerly case, $\omega_b/k\delta q = 0$, in contrast, there is such strong wave excitation on the equatorial wave guide that there is vigorous mixing on both flanks throughout the tropics and even across the wave guide itself. Mixing in this case is considerably more active that that normally observed in the winter lower-middle stratosphere.

Although waves are not propagating on a smooth background potential vorticity field, the Eliassen–Palm (EP) flux still provides a useful description of the flux of wave activity between regions. In the study of ES05, the only wave guide was the vortex edge and so the only relevant EP flux was the horizontally averaged vertical component of the full vector flux. Here because waves can transfer horizontally between wave guides it is also meaningful to consider the vertically averaged horizontal component. This is shown in Fig. 9 for the easterly and westerly perturbation cases, again with $h_b = 0.2$ and $\omega_b/k\delta q \approx 0.0234$, at different times during the simulations. In both cases, the flux of wave activity from the polar vortex edge to the tropics is clear. In the easterly case the flux ends very close to ϕ_N, consistent with the above observation that the there is very little mixing across the tropics and relatively weak excitation of waves at ϕ_S. Note that the flux between ϕ_N and ϕ_S can have no convergence, i.e. the horizontal gradient of the vertical average must be zero, since there is no possibility of wave activity being deposited in this region, with zero potential vorticity gradient. The small

flux across the tropics therefore represents the weak remote transfer of wave activity from ϕ_N to ϕ_S. Note that the distance between ϕ_N and ϕ_S is approximately the same as the distance between ϕ_v and ϕ_N; the stronger flux between the latter wave guides again illustrates the ability of the finite amplitude vortex disturbance to bridge the gap.

In the westerly case, the flux of wave activity from the polar vortex edge ends at the equatorial wave guide. In between, the flux is approximately uniform in latitude, again reflecting the lack of wave absorption in this region. South of the equator, there is a secondary transfer to ϕ_S, with approximately uniform flux inbetween. South of ϕ_S there is more gradual attenuation of the flux as wave activity is absorbed more continuously by the background planetary potential vorticity. The pattern of horizontal fluxes is entirely consistent with the structure of potential vorticity mixing shown in Fig. 8.

4.3. Role of vertical structure

The vertically uniform tropical potential vorticity perturbations used in the preceding discussion were chosen for simplicity and to focus on the main effect of these anomalies on the vortex response and wave propagation. Wind anomalies in the tropical stratosphere associated with the QBO are of relatively shallow extent and it is interesting to ask what if any of the above effects persist with shallow anomallies. To address this, we repeat the above perturbation experiments, but with the perturbations (5) and (6) limited in vertical extent to between $z = H$ and $z = 3H$. On other vertical levels the initial potential vorticity distribution is identical to that of the control, given by (4). This is not intended to resemble the QBO in any realistic way but simply to consider briefly the effect of finite vertical scale of the anomaly.

The vortex response obtained with these perturbations is shown in Fig. 10. As before, there is a reduction in the vortex response under the easterly anomaly and an enhancement of the response under the westerly anomaly. However, the magnitude of the difference in response to the vertically localized perturbations is significantly less than to the vertically uniform perturbations (compare Fig. 4). This is perhaps to be expected: in terms of angular momentum or circulation, the vertically localized perturbations are much smaller than those of the preceding section.

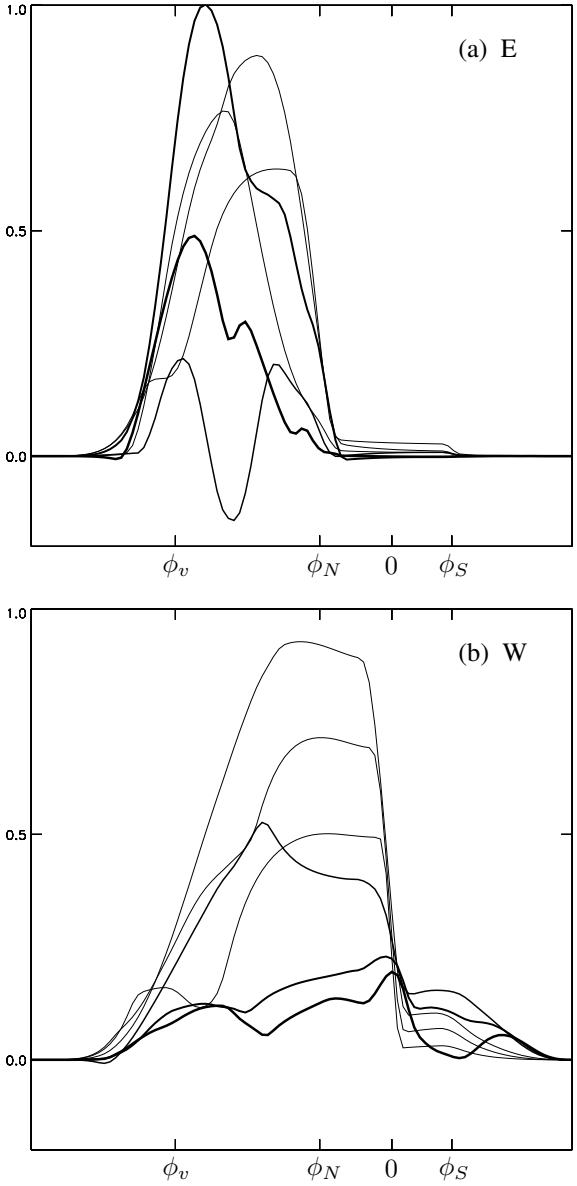

Figure 9. Vertically average of the horizontal component of EP flux at $t = 0$–$t = 5$ days, at daily intervals, for the cases shown in Fig. 8: (a) easterly perturbation (b) westerly perturbation. Later times are drawn with increasing line thickness. Positive values indicate flux towards the equator.

The tropical response for the same cases is shown in Fig. 11. Again, both cases are closer to the control case than the cases with uniform-in-height perturbations. The peak tropical response is very slightly enhanced in the westerly cases, more especially at the larger forcing amplitudes. Inspection of the potential vorticity at the mid-level of the perturbation (not shown), reveals similar behaviour to

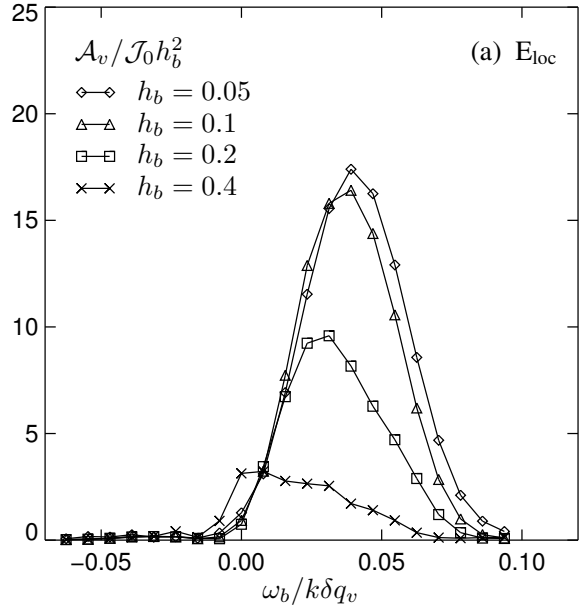

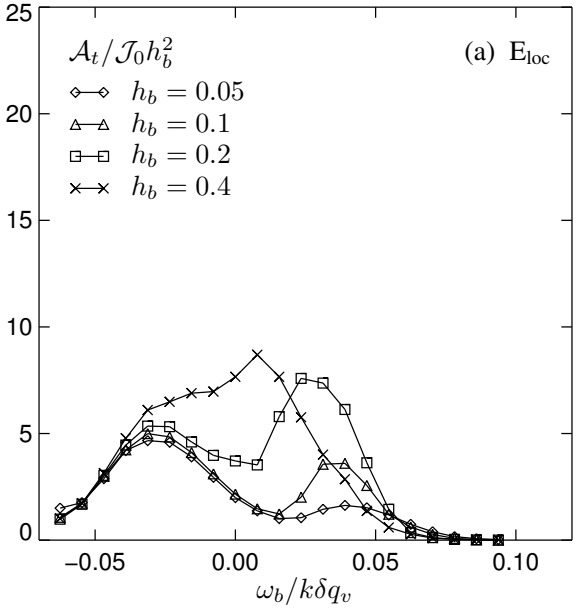

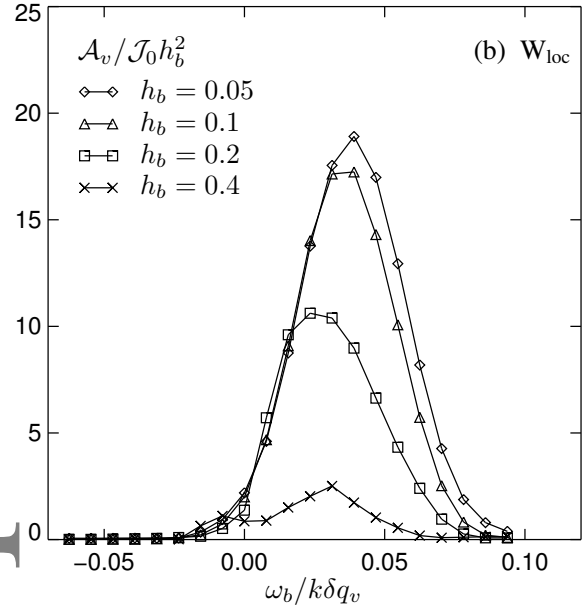

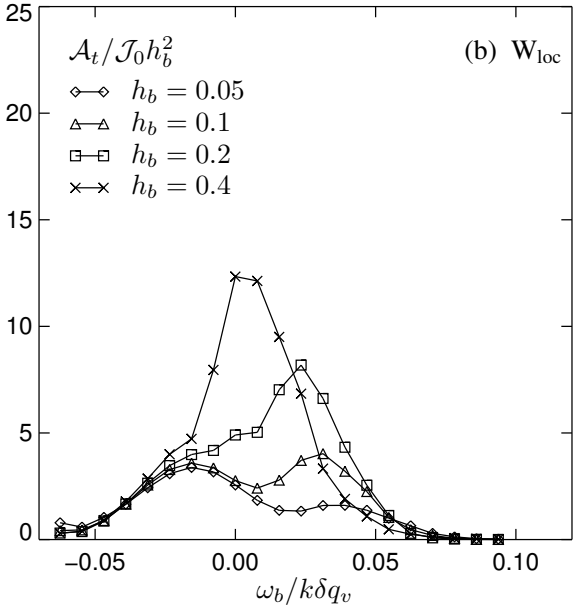

Figure 10. Vortex response, as Fig. 4 but for tropical anomalies that are localized in the vertical in the range $H \leq z \leq 3H$

Figure 11. Tropical response, as Fig. 6 but for tropical anomalies that are localized in the vertical in the range $H \leq z \leq 3H$

that seen in Fig. 8: in the easterly case, the potential vorticity jump at ϕ_N is advected and mixed into the surf zone, whereas in the westerly case, the equatorial potential vorticity jump is largely undular but tracer mixing within the tropics more widespread. That the peak should be strongest for the westerly case is perhaps surprising because the tropical potential vorticity is more distant from the polar vortex edge. However, the transfer of wave activity is more complicated here owing to the presence of background potential vorticity gradients throughout the tropics at other vertical levels; EP fluxes (not shown) indicate significant vertical propagation within the tropical region itself

We conclude with a brief look at the zonal mean flow changes associated with the transfer of wave activity to the tropics. Figure 12 shows differences in total vortex deceleration between the perturbation and control experiments. The total deceleration is defined simply as the difference in zonal mean zonal velocity between initial and final times:

$$\Delta\bar{u}(\phi, z) = \bar{u}(\phi, z; t = 10) - \bar{u}(\phi, z; t = -10).$$

This is computed for the control case and for both perturbation experiments, giving $\Delta\bar{u}_C$, $\Delta\bar{u}_E$, and $\Delta\bar{u}_W$. The quantities plotted in the Figure are then $\Delta\bar{u}_E - \Delta\bar{u}_C$ (a) and $\Delta\bar{u}_W - \Delta\bar{u}_C$ (b). Shading corresponds to an enhanced deceleration of the flow relative to the control case, unshaded contours to a reduction of the deceleration.

First considering the changes to the vortex, we see that there is anomalously weak deceleration of the polar vortex in the easterly case, predominatly at levels of the tropical perturbation, but extending to some extent throughout the full depth of the domain. This is consistent with the reduction of vortex response already seen in the wave activity. In the westerly case, there is comparatively little change in the vortex deceleration from that of the control case, the only enhanced deceleration occuring at higher levels.

More substantial changes are found in the tropics. In the easterly case, there is anomalously weak deceleration in the tropical region, between the equator and ϕ_N. Here the initial perturbation is already easterly, and potential vorticity is zero. It is therefore difficult to rearrange potential vorticity into a more easterly state. More deceleration occurs in the control case, resulting in a positive anomaly. Just north of ϕ_N, on the other hand, there is marked anomalous deceleration, consistent with the mixing of potential vorticity out of the tropical region and into the surf zone. The effect of the planetary waves in this case is therefore to extend the easterly perturbation to the north of the tropical region.

In the westerly case, the opposite pattern is found. At the level of the perturbation, there is anomalously strong deceleration on the equator, associated with the increase in wave activity of the equatorial wave guide. At the northern edge of the tropics, near ϕ_N the deceleration is weaker than in the control case, which exhibits mixing of the nonzero planetary vorticity gradients there. Interestingly, there is enhanced deceleration of the westerly case in the latitude range $0 < \phi < \phi_N$ at levels above and below the perturbation. Deceleration on these levels is due to enhanced mixing of the planetary potential vorticity, here given initially by the control profile. The wave transfer to the equatorial wave guide, though localized in height, therefore has a nonlocal-in-height effect. Inspection of EP flux cross-sections (not shown) indicates vertical propagation of waves within the equatorial region, both upward and downward out of the westerly zone. The pathway is thus lateral transfer of wave activity from the polar vortex to the equatorial wave guide in a shallow vertical range coinciding with the QBO westerlies, followed by vertical wave propagation out of the westerly region on the background planetary vorticity gradient.

5. Conclusions

We have presented a simplified picture of latitudinal wave transfer that is in some sense complementary to the traditional one where there is a clear scale separation between background flow and wave perturbations. It is a nonlocal transfer, involving the global nature of potential vorticity inversion, which for a fixed distance between wave guides and small amplitude waves can be described by a linear response function. When waves assume a finite amplitude, however, to the extent that the distance between wave guides is altered locally, the transfer becomes fully nonlinear, both in terms of response amplitude and zonal wavenumber. The enhanced proximity of one wave guide to the other in the locality of the wave crest implies a larger induced perturbation on the secondary wave guide over a confined range of longitudes. This effect will be further accentuated by a cylindrical or spherical geometry. In the winter stratosphere, where undulations of the vortex edge are significant, this situation may be relevant more often than not. On the other hand, our picture presupposes well defined wave guides, which may be less appropriate in the early winter, before the vortex edge has been sharpened by wave erosion.

The results of the numerical experiments support the conceptual picture and, in particular, illustrate the superlinear scaling of wave transfer from the vortex edge

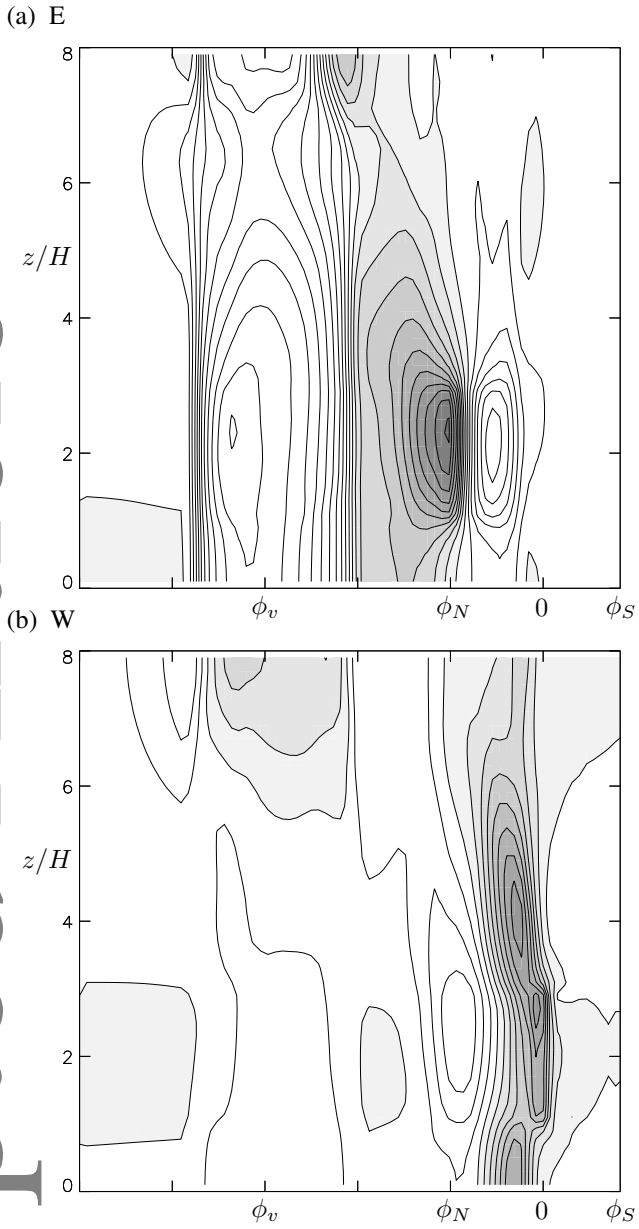

Figure 12. Deceleration difference between the perturbation and control experiments, (a) $\Delta\bar{u}_E - \Delta\bar{u}_C$ and (b) $\Delta\bar{u}_W - \Delta\bar{u}_C$, for the two cases shown in Fig. 10. See text for details. Contour interval is 1 ms^{-1}; negative values (anomalous deceleration) are shaded.

to the tropical wave guide: wave activity in the tropics increases with increasing forcing amplitude well beyond what would be expected from linear propagation. Both the enhanced transfer and the shift to higher zonal wavenumber is also visible in snapshots of the potential vorticity field.

One of the original motivations for the particular model configuration used here, in particular the forms of easterly and westerly tropical anomalies, was as a simplified system in which to investigate the Holton-Tan effect, the observed correlation between QBO phase and strength of the winter vortex. The remarks made in the introduction concerning the deep vertical scale of waves on the vortex edge and lack of scale separation can be extended to include the relatively shallow vertical extent of the QBO wind anomalies. A satisfactory explanation of the Holton-Tan effect should take into account the long-wavelength, finite amplitude nature of the waves as well as the inhomogeneities in the background mean flow. The present paper was partly conceived as a way to explore these ideas.

In the numerical experiments presented, there is a modest difference in the vortex response to easterly and westerly tropical anomalies, particularly for anomalies that are uniform in height but also, though to a much weaker extent, for those confined to the lower part of our model stratosphere. However, the vortex response to the tropical anomaly is in the opposite sense to that of the Holton-Tan effect, the easterly anomaly resulting in a lower vortex response than the westerly one. It thus appears that the current framework is insufficient to address this effect. Modulation of the transfer of wave activity from the polar vortex edge to the tropics is only one machanism in which the tropical circulation may affect the vortex evolution; clearly there are many potentially important factors not included in the model, such as vertical phasing or the seasonal cycle. The difference in the tropical potential vorticity between easterly and westerly anomalies implies, for example, a difference in the latitudinal structure of the wave modes of the vortex edge and therefore their projection onto the topographic forcing. Perhaps more importantly, as pointed out in Anstey and Shepherd (2014), the Holton-Tan response is strongest in early winter, when wave dynamics may be very different from that presented here. Finally, the recent analysis of White *et al.* (2015) suggests that a full explanation of the Holton-Tan effect requires consideration of the mean meridional circulation of the QBO easterly phase and its effect on the position of the subtropical jet, neither of which exist in the present model, though the latter could potentially be included following Esler *et al.* (2006). We conclude that, while the present model may eventually be able to shed some

light on the observed correlation between QBO phase and vortex response, it will require a more refined analysis and interpretation.

Two remaining results are worth noting, both concerning the tropical rather than the polar response. First, as was seen in Fig. 12, there is a small but clear difference in the structure of mean flow deceleration anomlies betweeen the easterly and westerly cases. If we interpret the vertically localized easterly and westerly initial conditions as proxies for QBO easterly and westerly phases, then the above results suggest that planetary wave forcing from midlatitudes may act to extend an easterly anomaly beyond the tropics and into the winter hemisphere. In contrast, its effect on the westerly anomaly is that of a reduction in the wind maximum on the equator. The extent to which these effects may combine with forcing of the QBO by tropical waves is an open and potentially interesting question.

Second, although the tropical response, as measured by the wave activity, is broadly similar between the easterly and westerly cases (Figs. 6 and 11) the nature of the accompanying mixing is markedly different. Entrainment of tropical air into the surf zone in the easterly case is limited to air from very close to the subtropical barrier at ϕ_N, while in the westerly case involves air from the entire region north of the equator, as well as local mixing on the southern side. The character of the mixing found here is broadly consistent with previous analysis of effective diffusivity in reanalysis datasets. The present results give a more detailed view of the mixing from a Lagrangian perspective and indicate a direction of transport predominantly out of the tropics.

Acknowledgements

Partial support for this work was provided through the National Science Foundation award AGS-1333029.

References

Abalos M, Randel WJ, Birner T. 2016. Phase-speed spectra of eddy tracer fluxes linked to isentropic stirring and mixing in the upper troposphere and lower stratosphere. *J. Atmos. Sci* **73**: 4711–4730.

Albers JR, Birner T. 2014. Vortex preconditioning due to planetary and gravity waves prior to stratospheric sudden warmings. *J. Atmos. Sci.* **71**: 4028–4054.

Andrews DG, Holton JR, Leovy CB. 1987. *Middle Atmosphere Dynamics*. Academic Press.

Anstey A, Shepherd TG. 2014. High-latitude influence of the quasi-biennial oscillation. *Q. J. Roy. Meteorol. Soc.* **140**: 1–21.

Dritschel DG, Ambaum MHP. 1997. A contour-advective semi-Lagrangian numerical algorithm for simulating fine-scale conservative dynamical fields. *Q. J. Roy. Meteorol. Soc.* **123**: 1097–1130.

Dritschel DG, McIntyre ME. 2008. Multiple jets as PV staircases: the Phillips effect and the resilience of eddy-transport barriers. *J. Atmos. Sci* **65**: 855–874.

Dritschel DG, Saravanan R. 1994. Three-dimensional quasi-geostrophic contour dynamics, with an application to stratospheric vortex dynamics. *Q. J. Roy. Meteorol. Soc.* **120**: 1267–1297.

Dunkerton TJ. 1991. Nonlinear propagation of zonal winds in an atmosphere with Newtonian cooling and equatorial wavedriving. *J. Atmos. Sci.* **48**: 236–263.

Dunkerton TJ, Scott RK. 2008. A barotropic model of the angular momentum conserving potential vorticity staircase in spherical geometry. *J. Atmos. Sci.* **65**: 1105–1136.

Esler JG, Polvani LM, Scott RK. 2006. The Antarctic stratospheric sudden warming of 2002: A self-tuned resonance? *Geophys. Res. Lett.* **33**: L12 804.

Esler JG, Scott RK. 2005. On the excitation of transient Rossby waves on the polar stratospheric vortex and the barotropic sudden warming. *J. Atmos. Sci.* **62**: 3661–3682.

Holton JR, Tan HC. 1982. The quasi-biennial oscillation in the northern hemisphere lower stratosphere. *J. Meteorol. Soc. Japan* **60**: 140–148.

Juckes MN, McIntyre ME. 1987. A high resolution, one-layer model of breaking planetary waves in the stratosphere. *Nature* **328**: 590–596.

Karoly D, Hoskins BJ. 1982. Three dimensional propagation of planetary waves. *J. Meteorol. Soc. Japan* **60**: 109–123.

Liu YS, Scott RK. 2015. The onset of the barotropic sudden warming in a global model. *Q. J. Roy. Meteor. Soc.* : doi: 10.1002/qj.2580.

Macaskill C, Padden WEP, Dritschel DG. 2003. The CASL algorithm for quasi-geostrophic flow in a cylinder. *J. Comput. Phys.* **188**: 232–251.

Matsuno T. 1970. Vertical propagation of stationary planetary waves in the winter northern hemisphere. *J. Atmos. Sci.* **27**: 871–883.

Matthewman NJ, Esler JG. 2011. Stratospheric Sudden Warmings as Self-Tuning Resonances. Part I: Vortex Splitting Events. *J. Atmos. Sci* **68**: 2481–2504.

Matthewman NJ, Esler JG, Charlton-Perez AJ, Polvani LM. 2009. A new look at stratospheric sudden warmings. Part III. Polar vortex evolution and vertical structure. *J. Clim.* **22**: 1566–1585.

Nakamura N, Solomon A. 2011. Finite-amplitude wave activity and mean flow adjustments in the atmospheric general circulation. Part II: analysis in the isentropic coordinate. *J. Atmos. Sci.* **68**: 2783–2799.

Nakamura N, Zhu D. 2010. Finite-amplitude wave activity and diffusive flux of potential vorticity in eddy–mean flow interaction. *J. Atmos. Sci.* **67**: 2701–2716.

Plumb RA. 1981. Instability of the distorted polar night vortex: a theory of stratospheric warmings. *J. Atmos. Sci.* **38**: 2514–2531.

Polvani LM, Waugh DW, Plumb RA. 1995. On the subtropical edge of the stratospheric surf zone. *J. Atmos. Sci.* **52**: 1288–1309.

Scott RK. 2016. A new class of vacillations of the stratospheric polar vortex. *Q. J. Roy. Meteor. Soc.* **142**: 1948–1957.

Scott RK, Dritschel DG, Polvani LM, Waugh DW. 2004. Enhancement of Rossby wave breaking by steep potential vorticity gradients in the winter stratosphere. *J. Atmos. Sci* **61**: 904–918.

Scott RK, Liu YS. 2015. On the formation and maintenance of the stratospheric surf zone as inferred from the zonally averaged potential vorticity distribution. *Q. J. Roy. Meteor. Soc.* **141**: 327–332.

Shuckburgh EF, Norton WA, Iwi AM, Haynes PH. 2001. Influence of the quasi-biennial oscillation on isentropic transport and mixing in the tropics and subtropics. *J. Geophys. Res* **106**: 14 327–14 337.

Simmons AJ. 1974. Planetary-scale disturbances in the polar winter stratosphere. *Q. J. Roy. Meteorol. Soc.* **100**: 76–108.

Tung KK, Lindzen RS. 1979a. A theory of stationary long waves. Part I: A simple theory of blocking. *Mon. Wea. Rev.* **107**: 714–734.

Tung KK, Lindzen RS. 1979b. A theory of stationary long waves. Part II: Resonant Rossby waves in the presence of realistic vertical shears. *Mon. Wea. Rev.* **107**: 735–750.

Waugh DW, Dritschel DG. 1999. The dependence of Rossby wave breaking on the vertical structure of the polar vortex. *J. Atmos. Sci.* **56**: 2359–2375.

White IP, Lu H, Mitchell NJ, Phillips T. 2015. Dynamical response to the QBO in the Northern winter stratosphere: signatures in wave forcing and eddy fluxes of potential vorticity. *J. Atmos. Sci* **72**: 4487–4507.

Zhu D, Nakamura N. 2010. On the representation of Rossby waves on the β-plane by a piecewise uniform potential vorticity distribution. *J. Fluid Mech.* **664**: 397–406.